BIOCHEMISTRY
including biophysical chemistry & molecular biology

Article

pubs.acs.org/biochemistry

Shift in the Equilibrium between On and Off States of the Allosteric Switch in Ras-GppNHp Affected by Small Molecules and Bulk Solvent Composition

Genevieve Holzapfel,[†] Greg Buhrman,[†] and Carla Mattos*[,†,‡]

[†]Department of Molecular and Structural Biochemistry, North Carolina State University, Raleigh, North Carolina 27695, United States

[‡]Department of Chemistry and Chemical Biology, Northeastern University, Boston, Massachusetts 02115, United States

Supporting Information

ABSTRACT: Ras GTPase cycles between its active GTP-bound form promoted by GEFs and its inactive GDP-bound form promoted by GAPs to affect the control of various cellular functions. It is becoming increasingly apparent that subtle regulation of the GTP-bound active state may occur through promotion of substates mediated by an allosteric switch mechanism that induces a disorder to order transition in switch II upon ligand binding at an allosteric site. We show with high-resolution structures that calcium acetate and either dithioerythritol (DTE) or dithiothreitol (DTT) soaked into H-Ras-GppNHp crystals in the presence of a moderate amount of poly(ethylene glycol) (PEG) can selectively shift the equilibrium to the "on" state, where the active site appears to be poised for catalysis (calcium acetate), or to what we call the "ordered off" state, which is associated with an anticatalytic conformation (DTE or DTT). We also show that the equilibrium is reversible in our crystals and dependent on the nature of the small molecule present. Calcium acetate binding in the allosteric site stabilizes the conformation observed in the H-Ras-GppNHp/NOR1A complex, and PEG, DTE, and DTT stabilize the anticatalytic conformation observed in the complex between the Ras homologue Ran and Importin-β. The small molecules are therefore selecting biologically relevant conformations in the crystal that are sampled by the disordered switch II in the uncomplexed GTP-bound form of H-Ras. In the presence of a large amount of PEG, the ordered off conformation predominates, whereas in solution, in the absence of PEG, switch regions appear to remain disordered in what we call the off state, unable to bind DTE.

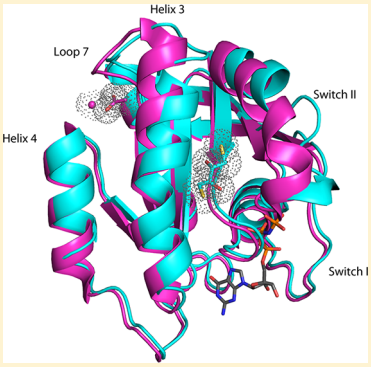

Ras is a small monomeric GTPase that functions as a molecular switch in signal transduction.[1,2] It is involved in cell proliferation, apoptosis, and multiple cellular functions that play critical roles in the tumorigenesis of a variety of human cancers.[3,4] It is therefore not surprising that Ras and its mutants have been the focus of numerous biochemical and cell biology studies[5−10] as well as structural biology experiments primarily using the GTP analogue GppNHp to produce the activated state.[11−17] Ras is anchored to the membrane via an isoprenyl group as well as other posttranslational modifications at the C-terminus[18,19] and is normally activated through cell surface receptors.[20] When bound to GTP, Ras propagates its signal by interacting with effector proteins such as Raf,[21] phosphoinositide-3-kinase (PI3K),[22] Ral guanine nucleotide dissociation stimulator (RalGDS),[23] NOR1A,[24] and others.[19] Once GTP is hydrolyzed to GDP on Ras, interaction with effectors is no longer favored and signaling is turned off. The levels of Ras-GTP are kept in check by the opposing actions of guanine nucleotide exchange factors (GEFs) that catalyze the loading of GTP[25] and of GTPase-activating proteins (GAPs) that increase the intrinsically slow GTPase activity of Ras for timely depletion of Ras-GTP.[26] The active site residues are situated primarily in so-called switch I, switch II, and the phosphate binding loop (P-loop) comprised of residues 30−40, 60−76, and 10−17, respectively.[27] Oncogenic mutations interfere with the ability of Ras to hydrolyze GTP, resulting in a prolonged signal that promotes uncontrolled cell growth.[4] RasG12V and RasQ61L have received the most attention for being two of the most frequent point mutants commonly found in human cancers.[28−30]

The accepted view of the Ras cycle implies the absolute necessity of GAPs in increasing hydrolysis rates in vivo, as the intrinsic hydrolysis rates measured in vitro are too slow to be biologically relevant.[8] However, it has been known for many years that the RasG12P mutant is insensitive to GAPs yet has a normal intrinsic hydrolysis rate and a nontransforming phenotype.[14] Furthermore, the effector protein Raf binds to Ras with an affinity that is ∼1000-fold greater than the affinities of GAPs for Ras, and GAP would have to displace Raf for binding.[31−33] This is not the case for effectors such as PI3K and RalGDS that have affinities comparable to that of GAP.[22,34] We have recently discovered an allosteric switch in Ras where binding of calcium acetate in crystals with *R*32 symmetry

Received: April 18, 2012
Revised: July 10, 2012
Published: July 30, 2012

   dx.doi.org/10.1021/bi300509j | *Biochemistry* 2012, 51, 6114−6126

promotes a shift of helix 3 and loop 7 (residues 87−104 and 105−109, respectively) toward helix 4 (residues 126−137) and an extensive H-bonding network that results in a disorder to order transition in the active site with placement of catalytic residue Q61 for catalysis ("on" state of the allosteric switch).[13] This is in contrast to the structure from similar crystals grown in calcium chloride where switch II is disordered, resulting in an incomplete active site ("off" state of the allosteric switch).[6] In our model, intrinsic hydrolysis is activated by ligand binding at the allosteric site in the presence of Raf and plays a role in the control of signaling through the Ras/Raf/MEK/ERK pathway, alleviating the need for GAPs to compete with Raf for attenuation of the signal. In this context, RasG12P is expected to function normally in the Ras/Raf/MEK/ERK pathway despite its insensitivity to GAPs, consistent with its normal phenotype.

Our model provides a new venue through which to understand the complexities of the structural biology of Ras and its associated function. It was developed using H-Ras as a representative Ras protein, as this isoform was used in all of the structural biology and biochemical experiments referenced herein. In the canonical crystal form with $P3_221$ symmetry,[35] the highly conserved switch I residue Y32 is turned away from the nucleotide as in the Ras/RasGAP complex, in what has been determined by ^{31}P NMR to be "state 1".[34,36] In the crystal form with $R32$ symmetry, switch I is stabilized by crystal contacts with Y32 near the nucleotide as observed in the structure of the Raps/Raf-RBD complex[37] and determined by NMR to be "state 2" in the Ras/Raf-RBD complex in solution.[34] This is the switch I conformation associated with intrinsic hydrolysis.[36] We have therefore based our proposed mechanism for the reaction on the Ras structure obtained from crystals with $R32$ symmetry.[13] In the context of this switch I conformation, the allosteric switch may be either on or off to modulate the conformation of switch II, and we capture either one of these substates of Ras-GppNHp by growing the crystals in calcium acetate (on) or calcium chloride (off).[5] Because switch II is unhindered by crystal contacts in the $R32$ crystal form, we have an excellent mimic of the Ras active site in the Ras/Raf complex, where switch II is not part of the binding interface.[21]

Although calcium acetate is clearly not a physiological ligand, we propose that the calcium acetate at the allosteric site in our crystals mimics a functional group associated with the headgroup of a membrane lipid, perhaps in the presence of calcium, as this site on Ras has been shown to interact with the membrane in the GTP-bound, but not GDP-bound, state.[38,39] We have found that in the on state of the allosteric switch with a fully ordered active site, Y32 is closed over the nucleotide partially overlapping the position of the GAP arginine finger in the Ras/RasGAP complex.[26] In our crystals, as in the complex with Raf-RBD, Y32 interacts with a water molecule (Wat189) that forms a bridge to the γ-phosphate of GTP. Q61 is positioned by the allosteric switch to interact with this same water molecule that could receive a proton and develop a partial positive charge near the $\beta-\gamma$ bridging oxygen atom of GTP to stabilize the dissociative transition state of the reaction.[40,41] We propose that Wat189, aided by Y32 and Q61, is therefore a critical element in Ras catalysis in the absence of GAP when the allosteric switch is on because of the binding of Raf at switch I and a membrane-associated ligand at the allosteric site. Although we have observed these structural changes associated with ordering of the active site in our crystals, we have been unable to measure the expected increase in the rate of hydrolysis for wild-type Ras in the presence of calcium acetate either in the absence or in the presence of Raf-RBD in solution.[13] This is most likely due to the fact that a salt bridge involving R135 on helix 4 and a symmetry-related molecule in the crystal may be mimicking in vivo stabilization of the allosteric binding site by a salt bridge between R135 and a membrane phospholipid.[38,39] A destabilized allosteric site in solution would limit intrinsic hydrolysis rate measurements in vitro to a state in which the allosteric switch is off for wild-type Ras. The idea that without interaction at the allosteric site the allosteric switch is normally off is consistent with the fact that disorder of the switch regions, and thus an incomplete active site, is seen in solution by NMR spectroscopy.[42] Nevertheless, vibrational spectroscopy studies in solution support the role of Q61 in stabilizing water in the active site during GTP hydrolysis, consistent with our proposed mechanism.[43]

Ras mutants commonly found in human cancers occur most frequently at position 12, 13, or 61.[29] Interestingly, rather than having a disordered switch II in the off state, the highly transforming Q61 mutants, including RasQ61L, have a well-ordered switch II structure stabilized in an anticatalytic conformation by a hydrophobic cluster of switch I and switch II residues that isolate the nucleotide from bulk solvent.[6] We call this the ordered off state. In contrast to the off state where catalysis is slow, the ordered off state has no measurable catalytic activity.[5,6] Interestingly, the G12V mutant does not adopt this conformation, and switch II is disordered in the off state, just as it is in the wild-type structure.[5] This structural difference between RasG12V and RasQ61L corresponds both to differences in intrinsic hydrolysis rates in the presence of Raf kinase and to differences in MEK and ERK phosphorylation levels in NIH-3T3 cells, particularly in the presence of a PI3K inhibitor that eliminates crosstalk effects to ERK due to Akt phosphorylation.[5] Taken together, these results suggest that modulation of the switch II conformation affects signaling through the Ras/Raf/MEK/ERK pathway. It is therefore of great interest to be able to affect this modulation with small molecules.

Here we use the H-Ras isoform to show that either dithioerythritol (DTE) or dithiothreitol (DTT) binds between helix 3 and switch II in crystals of the GTP-bound form, stabilizing the ordered off anticatalytic conformation of switch II in the wild-type protein. We show that the allosteric switch can be predictably modulated by soaking crystals of H-Ras-GppNHp in solutions containing either calcium acetate, which stabilizes the on state, or DTE or DTT, which stabilizes the ordered off state. Having previously found a binding site where ligands stabilize the on state,[13] we identify one here where DTE or DTT stabilizes the off state and show that when both sites are "empty" we can capture a mix of the on and off states of the allosteric switch in our crystals. Furthermore, the equilibrium between the two states is reversible, depending on the presence of molecules with opposing effects in the soaking solutions. This equilibrium, however, is significantly affected by the presence of PEG in the bulk solvent surrounding the crystals, with a clear correlation between the increase in the concentration of PEG and promotion of the ordered off conformation associated with the DTE/DTT binding pocket.

EXPERIMENTAL PROCEDURES

Protein Expression, Purification, and Crystallization. H-Ras 1−166 was expressed and purified as previously

dx.doi.org/10.1021/bi300509j | *Biochemistry* 2012, 51, 6114−6126

described[12] and is termed Ras hereafter. GDP was exchanged with GTP analogue GppNHp using the previously published procedure.[13] The final protein solution used for crystallization contained 20 mM HEPES (pH 7.5), 50 mM NaCl, 20 mM $MgCl_2$, and 10 mM DTE with a protein concentration of 10−15 mg/mL. Sitting drop crystallization trays were set with a protein concentration of 10−15 mg/mL. Crystals were grown at 18 °C for at least 1 week in sitting drops containing 5 μL of a protein solution and 5 μL of a reservoir solution. The reservoir solution was made in the following way. A 0.05% *n*-octyl β-D-glucopyranoside solution was made by adding *n*-octyl β-D-glucopyranoside to either 0.2 M $CaCl_2$ and 20% (w/v) PEG 3350 (PEG Ion Screen 7 from Hampton Research) (used for set 1 in Tables 1 and 3) or 0.2 M $Ca(OAc)_2$ hydrate and 20% (w/v) PEG 3350 (PEG Ion Screen 28 from Hampton Research) (used for set 2 in Tables 2 and 3). The reservoir solution was comprised of 500 μL of one of the solutions described above diluted with 100−200 μL of the protein buffer solution above (without the protein) and 0−150 μL of 50% (w/v) PEG 3350.

Soaks. Ras-GppNHp crystals grown in the presence of calcium chloride were originally transferred to a stabilization solution containing 10 mM HEPES (pH 7.5), 20 mM $NaCl_2$, 10 mM $MgCl_2$, 100 mM $CaCl_2$, 30% PEG 3350, and 30% PEG 400. This resulted in the first two structures in Table 1.

For the experiments showing modulation of the equilibrium between the substates, Ras-GppNHp crystals grown in the presence of calcium chloride (set 1) were transferred to a calcium chloride stabilization solution containing 10 mM HEPES (pH 7.5), 20 mM $NaCl_2$, 10 mM $MgCl_2$, 100 mM $CaCl_2$, and 30% PEG 3350. The crystals were allowed to soak for 60 min. Crystals grown in the presence of calcium acetate (set 2) were transferred to a calcium acetate stabilization solution consisting of 10 mM HEPES (pH 7.5), 20 mM NaCl, 10 mM $MgCl_2$, 100 mM $Ca(OAc)_2$, and 30% PEG 3350. These crystals were also allowed to soak for 60 min. These two initial soaking conditions were used to equilibrate crystals grown in different wells to the same starting condition before subsequent soaks with the various experimental conditions as described in Results. In summary, all of the soaks for this set of experiments included 10 mM HEPES (pH 7.5), 20 mM NaCl, 10 mM $MgCl_2$, and 30% PEG 3350. They differed in the presence or absence of 100 mM $CaCl_2$, 100 mM $Ca(OAc)_2$, 100 mM DTT, and 100 mM DTE. After soaking in the initial stabilization solutions for 60 min as described above, crystals were transferred to their final soaking conditions for 1−2 h. Single crystals were then placed in cryo-loops, dunked quickly in a solution containing 30% (v/v) glycerol under the soaking condition, and flash-frozen in liquid nitrogen for X-ray data collection.

Data Collection, Processing, and Structure Refinement. Data were collected at 100 K at the SER-CAT ID-22 and BM-22 beamlines at Advanced Photon Source (Argonne, IL). The X-ray wavelength was 1.0 Å with a crystal to detector distance of 150 mm. The exposure time varied from 1 to 10 s with an oscillation of 1° per frame. Data processing was performed using HKL2000. The coordinates with Protein Data Bank (PDB) entry 3K8Y[13] were used for phasing all of the structures in which the allosteric switch is on. The model used for phasing the structures soaked under the high-PEG conditions with a bound DTE is PDB entry 2RGE.[6] All other structures with the allosteric switch in the off state were phased with the high-resolution structure of DTE-bound Ras resulting from the high-PEG conditions. Rigid-body refinement was performed using PHENIX[44] with data cut at 2.5 Å. This was followed by refinement with simulated annealing starting at 2000 K with the high-resolution reflections included. Model building was performed using COOT.[45] PHENIX was used for refinement and generation of electron density maps.

Hydrolysis Experiments. The Raf-RBD (residues 52−131) plasmid was transformed into BL21 cells for protein expression. Cells were grown in LB medium containing ampicillin and induced with 1.0 mM IPTG. Cell pellets were stored at −80 °C. When needed for the hydrolysis experiments, pellets were resuspended in 20 mM HEPES (pH 7.0) and lysed, and Raf-RBD was purified using cation exchange chromatography in a HiLoad 26/10 SP Sepharose column (GE Healthcare). The Raf-RBD-containing fractions were pooled and concentrated to a volume of ∼10 mL before further purification with gel filtration on a HiPrep 26/60 S200 gel filtration column. Raf-RBD was concentrated to ∼5 mg/mL and used for the hydrolysis experiments, and the remainder of the protein was stored at −80 °C.

Ras protein was purified bound to GDP as previously described.[12] Ras-GDP was exchanged for γ-^{32}P-labeled GTP by the following procedure. Ras-GDP (5 μg) was incubated at 30 °C for 15 min in exchange buffer [50 mM Tris-HCl (pH 7.5), 50 mM NaCl, and 10 mM EDTA] with 2 μCi of γ-^{32}P-labeled GTP in a total volume of 100 μL. Immediately after the incubation, the exchange reaction mixture was passed over a prechilled P-6 nucleotide-binding column pre-equilibrated in hydrolysis buffer (50 mM Tris-HCl and 50 mM NaCl). The labeled Ras-GTP was then used immediately in hydrolysis experiments.

For the hydrolysis experiments, 3 μg of ^{32}P-labeled Ras-GTP was incubated at 30 °C with excess Raf-RBD (36 μg) with or without 300 mM DTE in hydrolysis buffer supplemented with 1 mM $MgCl_2$ to start the hydrolysis reaction, in a total volume of 300 μL. Immediately after the addition of $MgCl_2$, a 30 μL aliquot was added to 400 μL of prechilled stop buffer that consisted of 5% activated charcoal, 0.2 M HCl, 1 mM NaH_2PO_4, and 20% ethanol. The rest of the reaction mixture was then incubated at 30 °C, and at multiple time points, 30 μL aliquots were quenched in 400 μL of prechilled stop buffer and kept on ice. After the final time point, the samples were centrifuged at 10000*g* for 10 min in a tabletop centrifuge. Next, 200 μL of the supernatant solutions was added to scintillation vials containing 1.2 mL of scintillation cocktail (ScintiVerse II from Fisher Scientific), and the $^{32}P_i$ was quantified by scintillation counting. The counts were converted to percent hydrolysis in Excel by the formula (count − initial count)/(final count − initial count) × 100. The results were plotted in Kaleidograph and fit to the equation $y = A \times \exp[-(x - x_0)/t_0] + C$, following a method described by Shutes and Der.[46] Results of two independent experiments were averaged to obtain the reported turnover rates.

RESULTS

All of the experiments in this work were conducted with a C-terminally truncated construct of H-Ras that includes residues 1−166 (the catalytic domain). To establish the reversibility of the on and off states, we present a systematic series of soaking experiments, clearly demonstrating that whether we start with the on state or off state of the allosteric switch we are able to induce the full transition in both directions in our crystals, given a moderate amount of PEG in the bulk solvent.

Table 1. Data Collection and Refinement Statistics for Ras-GppNHp Structures of Crystals Grown with $CaCl_2$[a]

	PEG 400/$CaCl_2$ ordered off	PEG 400/$Ca(OAc)_2$ ordered off	set 1, $CaCl_2$ "mixed"	set 1, $CaCl_2$/DTE ordered off	set 1, $CaCl_2$/DTT ordered off	set 1, $Ca(OAc)_2$ on
			Data Collection			
space group	*R*32	*R*32	*R*32	*R*32	*R*32	*R*32
temperature (K)	100	100	100	100	100	100
cell dimensions						
a, *b*, *c* (Å)	88.52, 88.52, 134.06	87.41, 87.41, 133.47	89.03, 89.03, 135.21	88.09, 88.09, 133.90	88.21, 88.21, 134.14	88.82, 88.82, 134.78
α, β, γ (deg)	90, 90, 120	90, 90, 120	90, 90, 120	90, 90, 120	90, 90, 120	90, 90, 120
resolution (Å)	35−1.39 (1.41−1.39)	35−1.42 (1.44−1.42)	50−1.82 (1.85−1.82)	50−1.73 (1.76−1.73)	50−1.57 (1.60−1.57)	50−1.60 (1.66−1.60)
R_{sym} or R_{merge}	0.063 (0.796)	0.059 (0.335)	0.058 (0.793)	0.100 (0.737)	0.064 (0.295)	0.075 (0.681)
I/σ	55.6 (2.3)	65.1 (9.1)	49.1 (2.9)	33.2 (2.6)	52.7 (7.3)	19.7 (2.2)
completeness (%)	99.9 (98.4)	100 (100)	99.9 (100)	100 (100)	99.6 (92.9)	99.9 (99.3)
redundancy	10.1 (5.0)	10.9 (10.7)	10.9 (9.2)	10.8 (8.5)	10.9 (9.0)	6.6 (3.8)
			Refinement			
resolution (Å)	1.39	1.42	1.82	1.73	1.57	1.60
no. of reflections	39055	46257	17736	21703	27768	25192
R_{work}/R_{free}	18.07/19.63	17.07/18.88	15.92/19.41	16.94/19.76	15.77/17.90	17.89/20.26
no. of atoms	1494	1561	2720	1495	1561	1552
protein	1328	1345	2575	1328	1324	1317
GppNHp	1	1	1	1	1	1
acetate	0	0	0	0	0	1
DTT/DTE	1	1	0	1	2	0
Ca^{2+}/Mg^{2+}	2/2	4/3	2/2	1/3	3/2	2/2
water	161	159	109	165	184	195
B factor						
protein	19.4	14.5	28.8	20.3	15.7	24.7
GppNHp	12.2	8.98	23.9	13.6	10.6	18.6
acetate						28.67
DTE/DTT	43.5	35.5		53.6	36.4	
water	31.0	26.0	40.1	32.0	27.4	34.1
rmsd	2.03	2.04	4.84	2.09	2.94	2.75
bond lengths (Å)	0.008	0.007	0.008	0.007	0.008	0.008
bond angles (deg)	1.26	1.15	1.06	1.17	1.38	1.13
PDB entry	4DLR	3V4F	4DLS	4DLX	4DLY	4DLU

[a]Crystals were originally grown in the presence of calcium chloride. All soaking solutions contained 30% PEG 3350. Those structures resulting from soaks in the presence of an additional 30% PEG 400 are indicated by PEG 400, along with the presence of calcium chloride, calcium acetate, DTE, or DTT and a designation for the state of switch II. Values in parentheses are associated with the highest-resolution shell.

dx.doi.org/10.1021/bi300509j | *Biochemistry* 2012, 51, 6114−6126

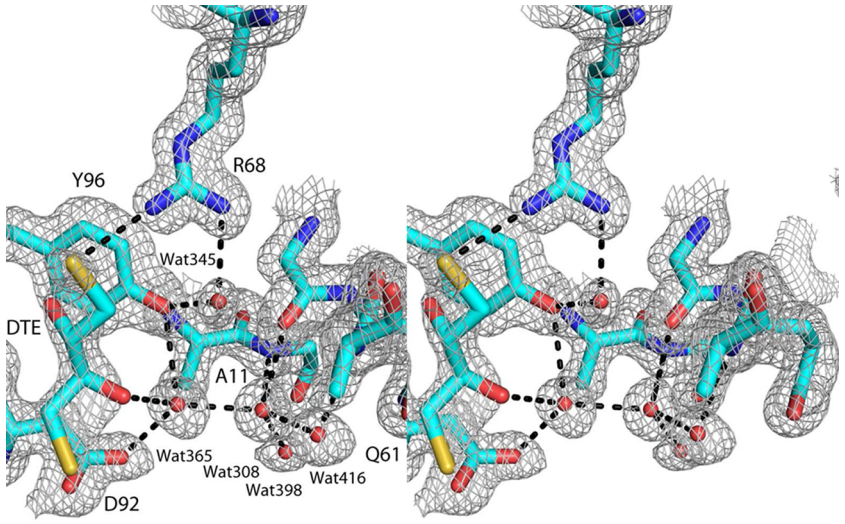

Figure 1. Binding pocket formed near the active site of Ras-GppNHp between helix 3 and switch II in the ordered off conformation, with a bound DTE molecule. Carbon atoms are colored cyan, nitrogen atoms blue, oxygen atoms red, and sulfur atoms yellow. The $2F_o - F_c$ electron density map contoured at the 1σ level is colored gray. Water molecules are represented by red spheres, and hydrogen-bonded atoms are connected by black dashed lines. This and all other stereoviews were made with a defocused representation.

DTE and DTT Bind in a Pocket between Switch II and Helix 3. When initially working out stabilization conditions for the soaks, we hit upon conditions under which the crystals were very stable and diffracted to a resolution of ~1.4 Å, higher than the resolution of 1.6−1.8 Å we usually get when we take crystals directly from the mother liquor. The condition contained 30% PEG 400 in addition to 30% PEG 3350 (vs 25% PEG 3350 in the mother liquor), as well as buffer and either calcium chloride or calcium acetate. As expected, we found that crystals originally grown in the presence of calcium chloride and 5 mM DTE and then soaked under the stabilization conditions containing 100 mM calcium chloride and no DTE had the allosteric switch in the off state (PEG 400/$CaCl_2$ ordered off in Table 1). Surprisingly, however, rather than a disordered switch II, we observed the ordered off conformation previously seen for the RasQ61L mutant.[6] Furthermore, this structure showed clear positive difference electron density in an $F_o - F_c$ electron density map contoured at 3σ, consistent with binding of DTE in a cleft that forms between helix 3 and the ordered off conformation of switch II in a position where we previously had located a hot spot for protein−ligand interaction using multiple-solvent crystal structure (MSCS) experiments.[11] Soaking of crystals in the high-PEG stabilization condition that included 100 mM $Ca(OAc)_2$ also gave an unexpected result. Rather than the on state of the allosteric switch, this structure showed the allosteric switch in the off state with switch II in the ordered off conformation [PEG 400/$Ca(OAc)_2$ ordered off in Table 1]. This structure too contained a bound DTE at the helix 3−switch II interface. It is clear that under the high-PEG conditions with bound DTE near the active site, the presence of 100 mM calcium acetate is not sufficient to promote the transition of the allosteric switch to the on state.

The DTE molecule in both structures binds in a pocket lined by Y96 from helix 3, with one of its two hydroxyl groups making a good H-bonding interaction with Wat365, which in turn H-bonds to the hydroxyl group of the tyrosine residue and to the side chain of D92 in helix 3 (Figure 1). Wat365 is part of a network involving Wat308 and the carbonyl group of G60, the residue immediately preceding the catalytic switch II residue Q61. Wat308 is highly conserved in the Ras structures and also makes H-bonding interactions to the main chain amide group of G12 in the P-loop and another water molecule, Wat416, that forms a bridge to the main chain amide of E62. This network of H-bonding interactions linking G60 to the DTE molecule results in a shift of the N-terminal portion of switch II in this structure relative to the off state in which switch II is disordered (PDB entry 2RGE). The DTE molecule is linked to the middle of switch II through one of its sulfur atoms that receives an H-bond from R68, which in turn interacts with Wat345 (Figure 1). Thus, through its interaction with R68, the DTE molecule is connected to both the hydroxyl group of Y96 in helix 3 and the carbonyl group of G60 in switch II. In essence, the DTE molecule interacts with elements of switch II, the P-loop, and helix 3 in the context of the ordered off conformation of switch II. Interestingly, R68 in the on state is central to the H-bonding interactions of the allosteric switch, leading to an ordered conformation of switch II.[13] The presence of DTE does not allow the positioning of R68 critical for the on state and at the same time optimizes interactions found in the ordered off state, favoring the anticatalytic conformation of the active site. The binding of DTT in this pocket has a very similar effect with only minor differences. There is a loss of H-bonding interaction between one of the DTT hydroxyl groups and Wat365 while its other hydroxyl group gains an H-bond with R68 (Figure S1 of the Supporting Information). The sulfur atom retains its interaction with R68 as in DTE.

The Active and Allosteric Sites Have Unique Conformations in the Ordered Off State. The binding of DTE or DTT with stabilization of switch II in the ordered off state results in an active site where residue Q61 participates in a hydrophobic pocket with switch I residues Y32, P34, and I36, as well as with switch II residue Y64, similar to that we observed previously for the Q61L, -I, -V, and -K mutants.[6] However, unlike the mutant residues that made van der Waals interactions within the active site, the polar portion of Q61 makes an excellent H-bonding interaction with the hydroxyl group of Y32, which also H-bonds directly to the γ-phosphate of the nucleotide (Figure 2). The γ-phosphate is, as usual, in

dx.doi.org/10.1021/bi300509j | *Biochemistry* 2012, 51, 6114−6126

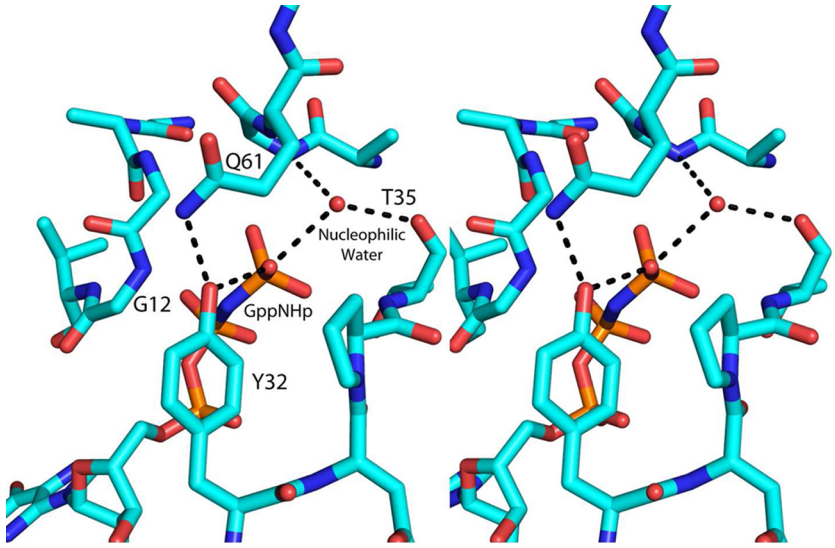

Figure 2. Active site of Ras-GppNHp in the ordered off conformation, including P-loop residues 10−14, switch I residues 32−35, and switch II residues 59−61. Carbon atoms are colored cyan, nitrogen atoms blue, and oxygen atoms, including the nucleophilic water molecule, red. Black dashed lines indicate hydrogen bonds. Note the direct interaction between Q61 and Y32.

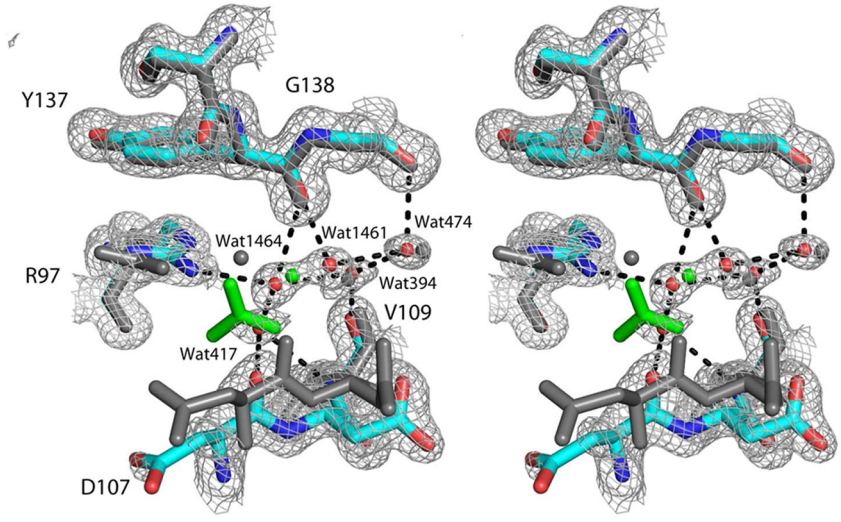

Figure 3. Allosteric site of Ras-GppNHp soaked in a high-PEG solution containing 100 mM calcium acetate. The labeling of protein residues and water molecules is pertinent to the structure in the ordered off state shown in color. For this structure, carbon atoms are colored cyan, nitrogen atoms blue, and oxygen atoms red. Water molecules are represented by red spheres, and hydrogen-bonded atoms are connected by black dashed lines. The associated $2F_o - F_c$ electron density map contoured at the 1σ level is colored light gray. Note the lack of electron density for calcium and acetate in the allosteric site, unlabeled in the figure, but colored green with the associated protein structure and water molecules colored gray (PDB entry 3K8Y).

the proximity of the nucleophilic water molecule. This conformation leaves no room for the bridging water molecule, Wat189, observed in the on state between Y32 and the γ-phosphate.[13]

The allosteric site has fewer water molecules in crystals soaked in the high-PEG solution with calcium chloride compared to the structure in a lower-PEG solution with a disordered switch II (PDB entry 2RGE). In the structure soaked in the high-PEG stabilization solution in the presence of 100 mM calcium acetate, crystallographic water molecules become more prominent in the allosteric site, with no visible binding of calcium acetate. In this structure, two water molecules (Wat1461 and Wat1464) interact with the carbonyl group of Y137 (Figure 3). These water molecules are too close to each other (1.9 Å) to be present simultaneously and are therefore not at full occupancy. Y137 interacts with Wat1464 in a manner reminiscent of its interaction with calcium ion in the on state. Wat1461 represents an alternate location for a similar interaction with Y137. Loop 7 is shifted toward switch II along with helix 3 in a way that is typical for the off state. This makes room for an additional water molecule, Wat417, to bridge between Wat1464 and the carbonyl group of D107 in a position that overlays well with the location of the acetate molecule present in the on state. Residue R97 is found in a conformation that would sterically clash with a bound acetate molecule, and it makes an H-bond to Wat1464. In this structure, R97 is in the same conformation found in the structures in the off state. However, there is weak positive electron density to support an alternate conformation of R97 similar to that found in the on state. In summary, an overall

dx.doi.org/10.1021/bi300509j | *Biochemistry* 2012, 51, 6114−6126

Table 2. Data Collection and Refinement Statistics for Ras-GppNHp Structures of Crystals Grown with $Ca(OAc)_2$[a]

	set 2, $Ca(OAc)_2$ on	set 2, $CaCl_2$/DTT ordered off	set 2, $Ca(OAc)_2$/DTT on	set 2, $Ca(OAc)_2$/DTE ordered off
		Data Collection		
space group	*R*32	*R*32	*R*32	*R*32
temperature (K)	100	100	100	100
cell dimensions				
a, *b*, *c* (Å)	88.70, 88.70, 134.36	88.82, 88.82, 134.05	88.40, 88.40, 133.92	88.26, 88.26, 134.40
α, *β*, *γ* (deg)	90, 90, 120	90, 90, 120	90, 90, 120	90, 90, 120
resolution (Å)	50−1.70 (1.76−1.70)	30−1.57 (1.63−1.57)	50−1.72 (1.75−1.72)	50−1.66 (1.69−1.66)
R_{sym} or R_{merge}	0.065 (0.865)	0.067 (0.827)	0.054 (0.666)	0.082 (0.654)
I/σ	21.0 (1.5)	37.3 (1.2)	49.3 (3.0)	39.4 (3.0)
completeness (%)	99.5 (95.0)	97.4 (79.8)	100 (100)	100 (100)
redundancy	7.9 (4.5)	9.6 (3.7)	10.4 (8.9)	11 (9.3)
		Refinement		
resolution (Å)	1.70	1.63	1.72	1.66
no. of reflections	20843	23884	20777	23146
R_{work}/R_{free}	17.77/20.05	19.48/21.74	17.41/20.24	16.17/18.42
no. of atoms	1502	1540	1529	1547
protein	1316	1320	1318	1378
GppNHp	1	1	1	1
aetate	1	0	1	0
DTT/DTE	0	1	0	2
Ca^{2+}/Mg^{2+}	2/2	3/1	2/2	2/3
water	146	176	171	161
B factor				
protein	29.9	23.2	26.8	19.4
GppNHp	22.4	16.2	19.8	13.4
acetate	37.28		35.56	
DTE/DTT		38.5		46.4
water	38.7	31.8	34.9	32.3
rmsd	3.31	3.23	2.83	3.56
bond lengths (Å)	0.008	0.008	0.007	0.007
bond angles (deg)	1.12	1.18	1.11	1.15
PDB entry	4DLT	4DLV	4DLW	4DLZ

[a]Crystals were originally grown in the presence of calcium acetate. All soaking solutions contained 30% PEG 3350. The presence of calcium chloride, calcium acetate, DTE, or DTT and a designation for the state of switch II are indicated. Values in parentheses are associated with the highest-resolution shell.

Table 3. Soak Conditions and Associated Structural Features of the Allosteric Switch in Ras-GppNHp

	structure	growth condition[a]	presoak condition[b]	final soak condition[b]	status of switch II[c]	bound small molecule or ion
set 1	$CaCl_2$ mixed	$CaCl_2$ with DTE	100 mM $CaCl_2$	same as presoak	mixed ordered on and disordered	none
	$CaCl_2$/DTE ordered off	$CaCl_2$ with DTE	100 mM $CaCl_2$	100 mM $CaCl_2$ with 100 mM DTE	ordered off	DTE in helix 3/switch II pocket
	$CaCl_2$/DTT ordered off	$CaCl_2$ with DTE	100 mM $CaCl_2$	100 mM $CaCl_2$ with 100 mM DTT	ordered off	DTT in helix 3/switch II pocket
	$Ca(OAc)_2$ ordered on	$CaCl_2$ with DTE	100 mM $CaCl_2$	100 mM $Ca(OAc)_2$	ordered on	calcium acetate in allosteric site
set 2	$Ca(OAc)_2$ ordered on	$Ca(OAc)_2$ with DTE	100 mM $Ca(OAc)_2$	same as presoak	ordered on	calcium acetate in allosteric site
	$CaCl_2$/DTT ordered off	$Ca(OAc)_2$ with DTE	100 mM $Ca(OAc)_2$	100 mM $CaCl_2$ with 100 mM DTT	ordered off	DTT in helix 3/switch II pocket
	$Ca(OAc)_2$/DTT ordered on	$Ca(OAc)_2$ with DTE	100 mM $Ca(OAc)_2$	100 mM $Ca(OAc)_2$ with 100 mM DTT	ordered on	calcium acetate in allosteric site
	$Ca(OAc)_2$/DTT ordered off	$Ca(OAc)_2$ with DTE	100 mM $Ca(OAc)_2$	100 mM $Ca(OAc)_2$ with 100 mM DTE	ordered off	DTE in helix 3/switch II pocket

[a]See Experimental Procedures for details of the crystal growth conditions for sets 1 and 2. [b]Components common to all soaks: 10 mM HEPES (pH 7.5), 20 mM NaCl, 10 mM $MgCl_2$, and 30% PEG 3350. [c]Switch I is always ordered in our crystals, stabilized by crystal contacts in the conformation found in the Ras/Raf complex.

comparison between the on state in the presence of 30% PEG 3350 and that of the ordered off state in the high-PEG solution in the presence of calcium acetate shows that the calcium ion and its three coordinating water molecules are replaced by two alternate positions for the interaction of water with the carbonyl of Y137 and a water molecule that connects it to the carbonyl

dx.doi.org/10.1021/bi300509j | *Biochemistry* 2012, 51, 6114−6126

group D107, which is positioned toward switch II, increasing the size of the allosteric site.

Equilibrium between On and Off States Modulated by Small Molecules in the Crystal. Given the prominence of the ordered off state in soaking solutions containing a high level of PEG (i.e., 30% PEG 3350 and 30% PEG 400) with the accompanying insensitivity to calcium acetate, the remaining experiments were conducted under the lower-PEG conditions (30% PEG 3350). We performed two sets of soaking experiments, one starting from the off state (set 1) and the other from the on state (set 2), to study the countering effects of calcium acetate and DTE or DTT in the transition between these two allosteric states in Ras-GppNHp crystals. The resulting structures are termed in the text as they are in Tables 1 and 2 containing the respective data collection and refinement statistics. In addition, Table 3 summarizes information regarding crystal growth, presoaking conditions [$CaCl_2$ or $Ca(OAc)_2$], soaking conditions (components that change in each soak), status of switch II (disordered, ordered on, or ordered off), and bound small molecule or ion. The first two structures in Table 1 correspond to those presented above (under the high-PEG conditions) and are not part of the present set of experiments. In the first set, set 1 in Tables 1 and 3, soaks were started from crystals containing Ras-GppNHp in the off state grown in the presence of calcium chloride and 1−5 mM DTE, which has a disordered switch II as previously observed (PDB entry 2RGE).[6] These crystals were transferred to a presoak stabilization solution containing 100 mM calcium chloride and no DTE, DTT, or calcium acetate, before a second transfer to solutions containing 100 mM calcium chloride and either 100 mM DTE or DTT, or 100 mM $Ca(OAc)_2$ without the reducing agents (Table 3). This set of soaks resulted in four structures with the data collection and refinement statistics listed in Table 1 (set 1). The structure from crystals transferred to a presoaking solution with calcium chloride but no DTE or DTT (set 1, $CaCl_2$ "mixed") shows electron density for both the on and off states of the allosteric switch, which were therefore both included in the refinement (Figure S2 of the Supporting Information). This is evidence that in the absence of calcium acetate and DTE or DTT, Ras is in equilibrium between the two states, sampled at detectable levels in our crystals. There is electron density for the entire switch II in the on state conformation as in our previously published structure bound to calcium acetate (PDB entry 3K8Y),[13] but no electron density for the N-terminal half of switch II in the off state, indicating that it is disordered as we previously observed in our structure in the presence of calcium chloride (PDB entry 2RGE).[6] Starting from switch II residue M67, there is electron density to support both the on and off states of the allosteric switch. The three other soaks belonging to set 1 were started from crystals of Ras that were presoaked in calcium chloride to attain this mixed structure. Addition of either 100 mM DTE (set 1, $CaCl_2$/DTE ordered off) or 100 mM DTT (set 1, $CaCl_2$/DTT ordered off) shifted the equilibrium toward the ordered off structure with clear electron density for a DTE/DTT in the switch II/helix 3 pocket. There is no visible electron density for the on state in these structures. Conversely, soaking in the presence of 100 mM $Ca(OAc)_2$ resulted in a structure with an equilibrium shift to the on state with no electron density to support the off state of the allosteric switch [set 1, $Ca(OAc)_2$ ordered on]. As expected, this structure has bound calcium and acetate at the allosteric site.

A second set of soaks, set 2 in Tables 2 and 3, was performed starting with crystals containing Ras-GppNHp in the on state grown in the presence of calcium acetate. These crystals were first transferred to a presoak solution containing 100 mM calcium acetate and no DTE or DTT [set 2, $Ca(OAc)_2$ ordered on]. Not surprisingly, this structure shows Ras with the allosteric switch in the on state and calcium acetate bound in the allosteric site. Transfer to a solution containing 100 mM calcium chloride and 100 mM DTT resulted in a structure that underwent a transition to the ordered off state with bound DTT near the active site (set 2, $CaCl_2$/DTT ordered off). Two additional soaks in this set were designed to explore the competition between binding of calcium acetate to promote the on state and DTE/DTT to promote the ordered off state. Ras-GppNHp crystals grown in the presence of calcium acetate and presoaked in a stabilization solution containing 100 mM $Ca(OAc)_2$ were then transferred to solutions containing either 100 mM $Ca(OAc)_2$ and 100 mM DTT [set 2, $Ca(OAc)_2$/DTT ordered on] or 100 mM calcium acetate and 100 mM DTE [set 2, $Ca(OAc)_2$/DTE ordered off]. Surprisingly, while the combination of calcium acetate and DTE resulted in a shift to the ordered off state with no bound calcium acetate in the allosteric site and DTE bound in the pocket between switch II and helix 3, the structure soaked in calcium acetate and DTT remained in the on state, with calcium acetate clearly bound in the allosteric site, the active site conformation ordered as previously observed (PDB entry 3K8Y),[13] and no electron density for DTT.

DTE Has No Effect on the Intrinsic Hydrolysis Rate of Ras in the Presence of Raf-RBD in Solution. Given that in the crystal the binding of DTE leads to the active site conformation observed for the RasQ61L mutant (PDB entry 2RGD) shown to be anticatalytic in the presence, but not in the absence, of Raf in solution,[6] we performed hydrolysis experiments to determine whether DTE results in a similar impairment of the rate of hydrolysis of GTP to GDP catalyzed by Ras in the presence of Raf-RBD (residues 51−131). The binding of Raf-RBD stabilizes switch I in the conformation seen in the crystal critical for stabilization of both the ordered off[6] and ordered on[13] conformations of switch II. Furthermore, it is not expected to hinder binding of DTE because the pocket between switch II and helix 3 is not part of the Raf-binding interface on Ras.[21] Conversely, the binding of DTE as well as the state of the allosteric switch should not affect Raf-RBD binding, because the relevant conformation of switch I is independent of the state of switch II, helix 3, and loop 7, the essential elements of the allosteric switch in the GTP-bound form of Ras.[5] A first set of hydrolysis experiments in the absence of Raf-RBD showed no effect of DTE (not shown). This is not surprising, because an effect, if any, would only be expected in the presence of Raf-RBD with a stable switch I. Ras was therefore loaded with [γ-^{32}P]GTP and the reaction allowed to proceed in the presence of Raf-RBD with and without 300 mM DTE. Aliquots were removed at multiple time points, and the extent of hydrolysis measured as described in Experimental Procedures. Single-turnover experiments in the absence of DTE resulted in the hydrolysis rate for wild-type Ras in the presence of Raf-RBD of 0.022 ± 0.001 min^{-1}, equivalent to a k_{cat} of 0.00037 ± 0.00002 s^{-1}, consistent with the previously published rate for this reaction[36] (Figure S3 of the Supporting Information). The turnover rate in the presence of 300 mM DTE is unchanged at 0.023 ± 0.003 min^{-1}, equivalent to a k_{cat} of 0.00038 ± 0.00005 s^{-1}, clearly establishing that DTE in

dx.doi.org/10.1021/bi300509j | Biochemistry 2012, 51, 6114−6126

solution does not affect the rate of intrinsic hydrolysis catalyzed by Ras, even in the presence of Raf and at a relatively high DTE concentration compared to that present in the crystal soaks (300 mM DTE in solution vs 100 mM DTE in the crystal).

DISCUSSION

Allosteric mechanisms were originally described for oligomeric or multidomain proteins where allosteric changes induced by ligand binding involve changes in quaternary structure or interdomain interactions.[47] More recently, the definition of allostery has been expanded to include ligand-induced changes in tertiary structure and the distribution of conformational ensembles within a monomeric protein.[48,49] It has become increasingly clear with our work and that of others that Ras-GTP (as modeled by Ras-GppNHp) is a monomeric protein regulated by shifts in conformational ensembles,[5,13,36,50] dynamically sampled in solution as shown for H-Ras-GppNHp[36,51,52] and K-Ras-GppNHp.[11,53] Here we have explored the shifts in equilibrium between conformational states modulated by the binding of small molecules in Ras-GppNHp crystals. We showed that calcium acetate and DTE/DTT can effectively promote conformational shifts to the on and off states of the allosteric switch, respectively, and we discovered that PEG in the bulk solvent has a dramatic effect on this process. Although these molecules are not physiologically relevant, they illustrate the possible modulation of conformational changes in Ras by competing elements in the cell, i.e., protein, membrane components, or small ligands binding at key sites on the protein surface. Furthermore, the effect of PEG serves as a reminder that the behavior of Ras isolated in dilute solutions may be different from that found in the crowded environment of the cell.[54]

We had previously identified the binding of calcium and acetate at the allosteric site as promoting a network of H-bonding interactions associated with the on state that culminate in the ordering of switch II with placement of Q61 in the catalytic center.[13] This structure has switch I and two active site water molecules as seen in the Raps/Raf complex.[37] Here we have identified DTE/DTT as binding near the active site in the ordered off state where switch II in wild-type Ras-GppNHp adopts the anticatalytic conformation we previously observed for the RasQ61L-GppNHp mutant. This site coincides with the most prominent binding site hot spot identified through our MSCS experiments and predicted by FT-Map calculations to be a druggable site.[11] This is an indication that the site could be a binding pocket for a natural ligand of Ras, although such a ligand has not yet been identified. Significantly, it is a site of interaction between the GTPase Ran in the GTP-bound form and Importin-β, where switch II is also found in the ordered off conformation with the physiological consequence of preventing GTP hydrolysis on Ran while cargo is being transported across the nuclear membrane.[55] In this structure, as in our structure of wild-type Ras-GppNHp in the ordered off conformation, both the γ-phosphate and switch II residue Q69 (Q61 in Ras) make direct hydrogen bonds with the hydroxyl group of Y32 and the two proteins have identical active site features.

PEG Affects Hydration of the Allosteric and Active Sites and Promotes Binding of DTE/DTT to Ras-GppNHp Crystals in the Off State. It is clear from the experiments presented here that the presence of PEG under the conditions in which Ras-GppNHp crystals are soaked has an effect on the structure and hydration of the two binding sites discussed in this work. There is a decrease in the number of water molecules in the allosteric site in crystals soaked in the high-PEG solution containing calcium chloride (PEG 400/$CaCl_2$ ordered off in Table 1) compared to the analogous structure in the lower-PEG solution (PDB entry 2RGE). This is due to a decrease in the level of protein hydration associated with the presence of 60% total PEG. This allosteric site dehydration effect is somewhat relieved in the structure soaked in high-PEG stabilization solution in the presence of calcium acetate [PEG 400/$Ca(OAc)_2$ ordered off in Table 1], although there is neither calcium nor acetate bound in this structure as shown in Figure 3. This could be due to preferential interaction of the acetate molecules with PEG in the bulk solvent, relieving the protein dehydration effect and at the same time making fewer acetate molecules available for interaction at the allosteric site.

The active site is also affected by the presence of PEG in the crystal soaking solutions. It is immediately apparent that the concentration at which either DTE or DTT is bound in the resulting structure is very sensitive to the bulk solvent composition. Whereas in the high-PEG soaks DTE/DTT is bound under all of our experimental conditions, the lower-PEG soaks require a higher concentration of DTE/DTT for it to bind in the crystal. Furthermore, under the lower-PEG conditions, calcium acetate binding at the allosteric site can compete with DTE/DTT between switch II and helix 3 near the active site, as our soaking experiments demonstrate. In solution where PEG is not present, we do not observe the expected reduced hydrolysis rate due to binding of DTE with stabilization of the ordered off anticatalytic conformation, even at a relatively high DTE concentration of 300 mM. This is consistent with the idea that DTE by itself is not able to select the ordered off conformation but instead binds at a binding pocket that is stabilized in the presence of PEG.

Our results show a correlation between stabilization of the ordered off conformation and an increasing concentration of PEG in the bulk solvent, which in turn facilitates binding of DTE/DTT. The effect is due to dehydration of the protein as the PEG concentration increases, resulting in a low water content at which the available water molecules preferentially interact with PEG. The switch regions contain several polar and charged groups that are normally well hydrated and either disordered in the off state of the allosteric switch or highly ordered in the on state with polar groups in extensive H-bonding interactions involving a large number of water molecules in the active site.[13] The ordered off conformation is characterized primarily by van der Waals and H-bonding interactions between protein atoms and between the protein and the nucleotide, with very few water molecules involved. The high-PEG condition promotes optimization of these H-bonding interactions, stabilizing the ordered off conformation of switch II, which in turn favors the binding of DTE/DTT to Ras even at very low concentrations. This is exemplified by our structure soaked in the high-PEG solution with 100 mM calcium acetate and no DTE/DTT. The original mother liquor in which Ras-GppNHp crystals were grown had only 1−5 mM DTE or DTT, but when transferred to the high-PEG solution with calcium acetate and no DTE/DTT, the allosteric site is "empty" and the DTE or DTT is bound with switch II in the ordered off conformation. The conditions under which the hydrolysis experiments were conducted in the absence of PEG represent the other extreme with a highly hydrated active site where switch II presumably remains disordered even at 300 mM DTE. The soaks in the solutions containing 30% PEG 3350 represent an intermediate state where DTE/DTT does

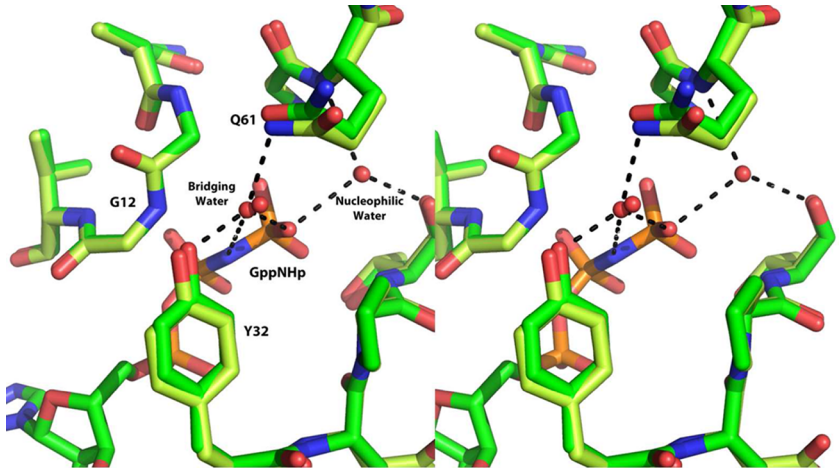

Figure 4. Active site superposition of Ras-GppNHp bound to calcium acetate in the on state of the allosteric switch (green) (PDB entry 3K8Y) and the Ras-GppNHp/NOR1A complex (yellow) (PDB entry 3DDC). The structures were superimposed solely on the basis of the nucleotide. In both cases, the bridging water molecule H-bonds with Y32, Q61, and the GppNHp and the nucleophilic water molecule H-bonds to the backbone amine and carbonyl groups of Q61 and T35, respectively, as well as to one of the γ-phosphate atoms of GppNHp. The hydrogen bonding interactions are shown as black dashed lines.

not bind in the low concentration range (1−10 mM), as exemplified by our previously published structure of Ras-GppNHp in the presence of calcium chloride,[6] but does bind at the higher DTE/DTT concentration of 100 mM. In summary, there is an effect of the PEG present in the bulk solvent surrounding the crystal that facilitates binding of DTE/DTT, which is absent under the solution conditions in which the hydrolysis experiments were performed. Interestingly, in a previously published attempt to correlate the ordered on conformation with enhanced catalysis, the expected increase in hydrolysis rate associated with binding of calcium acetate was not detected in solution,[13] in analogy to our current attempt to measure a decrease in hydrolysis rate with DTE in solution. As nonphysiological molecules, DTE, DTT, and acetate most likely interact with a low affinity at their respective binding sites on Ras-GppNHp and are unable to bind in dilute aqueous solutions. They do bind, however, aided by the more crowded environment of the crystal or by the effects of PEG on the bulk solvent, resulting in stabilization of conformations observed in biologically relevant complexes (see Discussion below). Physiological ligands would bind with higher affinities to these and other sites on Ras, stabilizing the relevant conformations, perhaps aided by the crowded environment of the cell.[54]

It is important to note that high-PEG solutions are not unique in stabilizing the ordered off conformation in Ras-GppNHp. In our MSCS experiments, soaks in four organic solvents at high concentrations were seen to have the same effect with a bound organic solvent molecule in place of the DTE/DTT: neat hexane, 60% 1,6-hexanediol, 55% dimethylformamide, and 50% 2,2,2-trifluoroethanol.[11] These solvents were previously observed to increase the level of order in switch II of Ras-GppNHp in the $P3_221$ crystal form by optimizing H-bonding interactions within protein atoms.[12] Within that crystal form, the N-terminal portion of switch II is disordered, but the C-terminal half is stabilized by crystal contacts to a conformation similar to that found in the Ras/RasGAP complex. The organic solvents order the N-terminal portion of switch II such that the entire switch superimposes well on switch II found in the complex with RasGAP.[12] In the *R*32 crystal form, where switch II is entirely away from crystal contacts, the ordered off conformation is stabilized with even more optimized protein interactions compared to that observed for the $P3_221$ crystal form, resulting in a pocket that can accommodate a variety of small molecules.[11]

The Active Site Conformation in the On State Is Associated with Tight Binding Effectors Raf and NOR1A. Our discovery of the allosteric switch in Ras-GppNHp crystals with *R*32 symmetry suggested a relevance to the interaction with Raf because this crystal form stabilizes a conformation of switch I identical to that seen in the Raps/Raf complex.[13] Furthermore, as in our crystals where switch II is free of crystal contacts, it is not part of the Ras−Raf interface. We subsequently established a connection between the allosteric switch and activation of the Ras/Raf/MEK/ERK signaling pathway in NIH-3T3 cells.[5] The major consequence of binding of calcium acetate at the allosteric site in our crystals is that it promotes an active site conformation in which the entire switch II, including catalytic residue Q61, becomes highly ordered. This structure is consistent with an intrinsic hydrolysis mechanism that stabilizes developing charges in the transition state through a bridging water molecule that interacts simultaneously with Q61, Y32, and the γ-phosphate of the nucleotide.[13] A slight increase in the intrinsic hydrolysis rate in the presence of Raf compared to uncomplexed Ras has been previously reported.[36] This is presumably due to ordering of switch I. We propose that this effect could be greatly enhanced by binding of membrane components at the allosteric site that promote the order of switch II through the allosteric switch mechanism in Raf-bound Ras.[11,13] Raf has a much higher affinity for Ras than do the effectors PI3K and RalGDS, with the Ras−Raf interaction having a K_d of 3.5 nM.[32] This would be tough competition for RasGAP, which has an affinity for Ras in the micromolar range[31] similar to those of PI3K[22] and RalGDS,[23] given that RasGAP would have to displace Raf to enhance the hydrolysis reaction. Intriguingly, a more recently discovered effector, NOR1A, also has an affinity for Ras in the nanomolar range, and the crystal structure of its complex with Ras-GppNHp is available in the literature.[24] Remarkably, the structure of the Ras-GppNHp/NOR1A complex (PDB entry 3DDC) has an active site identical to that observed in the on state of the allosteric switch in our crystals bound to calcium

dx.doi.org/10.1021/bi300509j | *Biochemistry* 2012, 51, 6114−6126

acetate (PDB entry 3K8Y and structures bound to calcium acetate presented here) (Figure 4). The switch I conformation is as in the Raps/Raf-RBD complex, and switch II makes interactions with an N-terminal extension of the NOR1A-RBD, through residues Y64 and M67, that stabilize the entire switch II in what we propose is the catalytic conformation for intrinsic hydrolysis in Ras. This supports the notion that the calcium acetate soaks presented here stabilize a biologically relevant conformation. NOR1A is a tumor suppressor protein that also interacts with the pro-apoptotic kinases MST1 and -2[56,57] and has been shown to colocalize with microtubules.[58,59] Not all of the functional consequences of its interaction with Ras are currently understood, but it has been shown that Ras binding is required for NOR1A's growth suppressor activities and that it leads to the inhibition of the ERK pathway.[60] Given the similarity of the Ras active site in the NOR1A complex with that in our structures with the allosteric switch in the on state, we propose that one mechanism through which NOR1A may exert its tumor suppressor properties is through enhancing hydrolysis of GTP on Ras, thus turning off Ras-mediated signaling through various pathways known to promote growth. The fact that both Raf and NOR1A, unlike other known Ras effectos such as PI3K and RalGDS, bind with affinities that are 3 orders of magnitude higher than the Ras/RasGAP affinity is consistent with the idea that these effectors may promote intrinsic hydrolysis under unique and tightly regulated conditions that do not involve RasGAP.

Relevance of the Ras-GppNHp Conformational Substates Associated with the Allosteric Switch. We have identified small molecules that have opposing effects with respect to the stabilization of substates in Ras-GppNHp found in functionally relevant protein complexes and have demonstrated the sensitivity of these substates to the bulk solvent conditions. Furthermore, we have shown that in the presence of a moderate amount of PEG it is possible to deliberately modulate the equilibrium between the two states in Ras-GppNHp crystals using calcium acetate bound at the allosteric site to stabilize the on state and either DTE or DTT bound near the active site between switch II and helix 3 to stabilize the off state. Both DTE/DTT and calcium acetate are associated with substates that have been previously observed either in Ras or in a homologous protein in complex with a biologically relevant binding partner. The DTE/DTT-bound ordered off conformation is identical to the conformation of Ran in complex with Importin-β, and it has been associated with a lack of catalysis both in the Ran complex[55] and in RasQ61L in the presence, but not in the absence, of Raf.[6] Binding of a protein or ligand at the site between switch II and helix 3 could render Ras incapable of hydrolyzing GTP with the consequence of prolonging active signaling in the cell. This would provide additional fine-tuning in the regulatory mechanisms that affect Ras signaling. The ordered on conformation associated with binding of calcium acetate in our crystals is the same as that observed in the Ras-GppNHp/NOR1A complex, with respect to both the on state of the allosteric switch and the conformational details of the active site formed by switch I and switch II residues. In addition, H-bonding networks, including the position of water molecules, are the same in the two structures. While NOR1A directly stabilizes this conformation, there appears to be an additional level of regulation in the complex with Raf, which stabilizes switch I leaving switch II to be modulated by ligand binding at the allosteric site near the membrane.[11,13,38,39] We propose that the off state structure obtained for crystals grown in calcium chloride with a disordered switch II is representative of the Ras-GTP/Raf complex in the absence of modulators, because in our crystals switch I is ordered as seen in the complex. This off state would be expected to be catalytically slow because of a disordered active site with only occasional access to the catalytic conformation. Binding at the allosteric site would activate the allosteric switch, promoting a shift in equilibrium to the on state, hydrolysis of GTP to GDP, and termination of signaling through the Ras−Raf interaction. Given that substates of Ras-GppNHp could be associated with levels of regulation more subtle than those provided by GAPs and GEFs, it is important to take them into account when targeting the activated state of Ras in the design of small ligands in the search for anticancer drugs.

■ ASSOCIATED CONTENT

Supporting Information

Figures S1−S3 and their figure legends. This material is available free of charge via the Internet at http://pubs.acs.org.

Accession Codes

Coordinates and structure factors have been deposited in the PDB as the entries listed in the last row of Tables 1 and 2 for each structure associated with this publication.

■ AUTHOR INFORMATION

Corresponding Author

*Department of Chemistry and Chemical Biology, Northeastern University, 102 Hurtig Hall, 360 Huntington Ave., Boston, MA 02115. Phone: (617) 373-6166. Email: c.mattos@neu.edu.

Notes

The authors declare no competing financial interest.

■ ACKNOWLEDGMENTS

Thanks to Bradley M. Kearney for writing an in-house program to renumber the water molecules in all of the structures presented in this paper so that they have the same numbering as in our recently published MSCS model (PDB entries 3RRY, 3RS2, 3RS7, 3RRZ, 3RSL, 3RSO, 3RS4, 3RS0, 3RS3, and 3RS5). Kathleen Davis, with guidance from Susan Fetics, made the construct of Raf-RBD (residues 52−131) from a construct of Raf-RBD-CRD (residues 52−184) previously used in the Mattos laboratory. Use of the Advanced Photon Source at the National Argonne Laboratory was supported by the U.S. Department of Energy, Office of Science, Office of Basic Energy Sciences, under Contract W-31-109-Eng-38.

■ ABBREVIATIONS

GppNHp, 5′-guanylylimidodiphosphate (a GTP analogue); PI3K, phosphoinositide-3-kinase; GEF, guanine nucleotide exchange factor; GAP, GTPase-activating protein; PEG, poly(ethylene glycol); DTE, dithioerythritol; DTT, dithiothreitol; Raps, Rap(E30D,K31E), Ras homologue Rap1A in which switch I residues E30 and K31 were mutated to D30 and E31, respectively, such that the switch I effector binding region has the sequence in Ras; rmsd, root-mean-square deviation.

■ REFERENCES

(1) Bourne, H. R., Sanders, D. A., and McCormick, F. (1990) The GTPase superfamily: Conserved switch for diverse cell functions. *Nature 348*, 125−132.

(2) Bourne, H. R., Sanders, D. A., and McCormick, F. (1991) The GTPase superfamily: Conserved structure and molecular mechanism. *Nature 349*, 117−127.
(3) Cox, A. D., and Der, C. J. (2003) The dark side of Ras: Regulation of apoptosis. *Oncogene 22*, 8999−9006.
(4) Karnoub, A. E., and Weinberg, R. A. (2008) Ras oncogenes: Split personalities. *Nat. Rev. Mol. Cell Biol. 9*, 517−531.
(5) Buhrman, G., Kumar, V. S., Cirit, M., Haugh, J. M., and Mattos, C. (2011) Allosteric Modulation of Ras-GTP Is Linked to Signal Transduction through RAF Kinase. *J. Biol. Chem. 286*, 3323−3331.
(6) Buhrman, G., Wink, G., and Mattos, C. (2007) Transformation efficiency of RasQ61 mutants linked to structural features of the switch regions in the presence of Raf. *Structure 15*, 1618−1629.
(7) Der, C. J., Finkel, T., and Cooper, G. M. (1986) Biological and biochemical properties of human rasH genes mutated at codon 61. *Cell 44*, 167−176.
(8) John, J., Schlichting, I., Schiltz, E., Rosch, P., and Wittinghofer, A. (1989) C-terminal truncation of p21H preserves crucial kinetic and structural properties. *J. Biol. Chem. 264*, 13086−13092.
(9) Neal, S. E., Eccleston, J. F., Hall, A., and Webb, M. R. (1988) Kinetic analysis of the hydrolysis of GTP by p21N-ras. The basal GTPase mechanism. *J. Biol. Chem. 263*, 19718−19722.
(10) Seeburg, P. H., Colby, W. W., Capon, D. J., Goeddel, D. V., and Levinson, A. D. (1984) Biological properties of human c-Ha-ras1 genes mutated at codon 12. *Nature 312*, 71−75.
(11) Buhrman, G., O'Connor, C., Zerbe, B., Kearney, B. M., Napoleon, R., Kovrigina, E. A., Vajda, S., Kozakov, D., Kovrigin, E. L., and Mattos, C. (2011) Analysis of Binding Site Hot Spots on the Surface of Ras GTPase. *J. Mol. Biol. 413*, 773−789.
(12) Buhrman, G., de Serrano, V., and Mattos, C. (2003) Organic solvents order the dynamic switch II in Ras crystals. *Structure 11*, 747−751.
(13) Buhrman, G., Holzapfel, G., Fetics, S., and Mattos, C. (2010) Allosteric modulation of Ras positions Q61 for a direct role in catalysis. *Proc. Natl. Acad. Sci. U.S.A. 107*, 4931−4936.
(14) Franken, S. M., Scheidig, A. J., Krengel, U., Rensland, H., Lautwein, A., Geyer, M., Scheffzek, K., Goody, R. S., Kalbitzer, H. R., Pai, E. F., et al. (1993) Three-dimensional structures and properties of a transforming and a nontransforming glycine-12 mutant of p21H-ras. *Biochemistry 32*, 8411−8420.
(15) Krengel, U., Schlichting, L., Scherer, A., Schumann, R., Frech, M., John, J., Kabsch, W., Pai, E. F., and Wittinghofer, A. (1990) Three-dimensional structures of H-ras p21 mutants: Molecular basis for their inability to function as signal switch molecules. *Cell 62*, 539−548.
(16) Tong, L. A., de Vos, A. M., Milburn, M. V., Jancarik, J., Noguchi, S., Nishimura, S., Miura, K., Ohtsuka, E., and Kim, S. H. (1989) Structural differences between a ras oncogene protein and the normal protein. *Nature 337*, 90−93.
(17) Tong, L. A., de Vos, A. M., Milburn, M. V., and Kim, S. H. (1991) Crystal structures at 2.2 Å resolution of the catalytic domains of normal ras protein and an oncogenic mutant complexed with GDP. *J. Mol. Biol. 217*, 503−516.
(18) Hancock, J. F. (2003) Ras proteins: Different signals from different locations. *Nat. Rev. Mol. Cell Biol. 4*, 373−384.
(19) Prior, I. A., and Hancock, J. F. (2012) Ras trafficking, localization and compartmentalized signalling. *Semin. Cell Dev. Biol. 23*, 145−153.
(20) Feig, L. A. (1993) The many roads that lead to Ras. *Science 260*, 767−768.
(21) Thapar, R., Williams, J. G., and Campbell, S. L. (2004) NMR characterization of full-length farnesylated and non-farnesylated H-Ras and its implications for Raf activation. *J. Mol. Biol. 343*, 1391−1408.
(22) Pacold, M. E., Suire, S., Perisic, O., Lara-Gonzalez, S., Davis, C. T., Walker, E. H., Hawkins, P. T., Stephens, L., Eccleston, J. F., and Williams, R. L. (2000) Crystal structure and functional analysis of Ras binding to its effector phosphoinositide 3-kinase γ. *Cell 103*, 931−943.
(23) Herrmann, C., Horn, G., Spaargaren, M., and Wittinghofer, A. (1996) Differential interaction of the ras family GTP-binding proteins H-Ras, Rap1A, and R-Ras with the putative effector molecules Raf kinase and Ral-guanine nucleotide exchange factor. *J. Biol. Chem. 271*, 6794−6800.
(24) Stieglitz, B., Bee, C., Schwarz, D., Yildiz, O., Moshnikova, A., Khokhlatchev, A., and Herrmann, C. (2008) Novel type of Ras effector interaction established between tumour suppressor NORE1A and Ras switch II. *EMBO J. 27*, 1995−2005.
(25) Boriack-Sjodin, P. A., Margarit, S. M., Bar-Sagi, D., and Kuriyan, J. (1998) The structural basis of the activation of Ras by Sos. *Nature 394*, 337−343.
(26) Scheffzek, K., Ahmadian, M. R., Kabsch, W., Wiesmuller, L., Lautwein, A., Schmitz, F., and Wittinghofer, A. (1997) The Ras-RasGAP complex: Structural basis for GTPase activation and its loss in oncogenic Ras mutants. *Science 277*, 333−338.
(27) Milburn, M., Tong, L., deVos, A. M., Brunger, A., Yamaizumi, Z., Nishimura, S., and Kim, S.-H. (1990) Structural Differences Between Active and Inactive Forms of Protooncogenic ras Proteins. *Science 247*, 939−945.
(28) Loupakis, F., Ruzzo, A., Cremolini, C., Vincenzi, B., Salvatore, L., Santini, D., Masi, G., Stasi, I., Canestrari, E., Rulli, E., Floriani, I., Bencardino, K., Galluccio, N., Catalano, V., Tonini, G., Magnani, M., Fontanini, G., Basolo, F., Falcone, A., and Graziano, F. (2009) KRAS codon 61, 146 and BRAF mutations predict resistance to cetuximab plus irinotecan in KRAS codon 12 and 13 wild-type metastatic colorectal cancer. *Br. J. Cancer 101*, 715−721.
(29) Prior, I. A., Lewis, P. D., and Mattos, C. (2012) A comprehensive survey of ras mutations in cancer. *Cancer Res. 72*, 2457−2467.
(30) Roberts, P. J., and Der, C. J. (2007) Targeting the Raf-MEK-ERK mitogen-activated protein kinase cascade for the treatment of cancer. *Oncogene 26*, 3291−3310.
(31) Martin, G. A., Viskochil, D., Bollag, G., McCabe, P. C., Crosier, W. J., Haubruck, H., Conroy, L., Clark, R., O'Connell, P., Cawthon, R. M., et al. (1990) The GAP-related domain of the neurofibromatosis type 1 gene product interacts with ras p21. *Cell 63*, 843−849.
(32) Minato, T., Wang, J., Akasaka, K., Okada, T., Suzuki, N., and Kataoka, T. (1994) Quantitative analysis of mutually competitive binding of human Raf-1 and yeast adenylyl cyclase to Ras proteins. *J. Biol. Chem. 269*, 20845−20851.
(33) Vogel, U. S., Dixon, R. A., Schaber, M. D., Diehl, R. E., Marshall, M. S., Scolnick, E. M., Sigal, I. S., and Gibbs, J. B. (1988) Cloning of bovine GAP and its interaction with oncogenic ras p21. *Nature 335*, 90−93.
(34) Geyer, M., Schweins, T., Herrmann, C., Prisner, T., Wittinghofer, A., and Kalbitzer, H. R. (1996) Conformational transitions in p21ras and in its complexes with the effector protein Raf-RBD and the GTPase activating protein GAP. *Biochemistry 35*, 10308−10320.
(35) Pai, E. F., Krengel, U., Petsko, G. A., Goody, R. S., Kabsch, W., and Wittinghofer, A. (1990) Refined crystal structure of the triphosphate conformation of H-ras p21 at 1.35 Å resolution: Implications for the mechanism of GTP hydrolysis. *EMBO J. 9*, 2351−2359.
(36) Spoerner, M., Hozsa, C., Poetzl, J. A., Reiss, K., Ganser, P., Geyer, M., and Kalbitzer, H. R. (2010) Conformational states of human rat sarcoma (Ras) protein complexed with its natural ligand GTP and their role for effector interaction and GTP hydrolysis. *J. Biol. Chem. 285*, 39768−39778.
(37) Nassar, N., Horn, G., Herrmann, C., Block, C., Janknecht, R., and Wittinghofer, A. (1996) Ras/Rap effector specificity determined by charge reversal. *Nat. Struct. Biol. 3*, 723−729.
(38) Abankwa, D., Hanzal-Bayer, M., Ariotti, N., Plowman, S. J., Gorfe, A. A., Parton, R. G., McCammon, J. A., and Hancock, J. F. (2008) A novel switch region regulates H-ras membrane orientation and signal output. *EMBO J. 27*, 727−735.
(39) Gorfe, A. A., Hanzal-Bayer, M., Abankwa, D., Hancock, J. F., and McCammon, J. A. (2007) Structure and dynamics of the full-length lipid-modified H-Ras protein in a 1,2-dimyristoylglycero-3-phosphocholine bilayer. *J. Med. Chem. 50*, 674−684.

(40) Du, X., Black, G. E., Lecchi, P., Abramson, F. P., and Sprang, S. R. (2004) Kinetic isotope effects in Ras-catalyzed GTP hydrolysis: Evidence for a loose transition state. *Proc. Natl. Acad. Sci. U.S.A. 101*, 8858−8863.
(41) Maegley, K. A., Admiraal, S. J., and Herschlag, D. (1996) Ras-catalyzed hydrolysis of GTP: A new perspective from model studies. *Proc. Natl. Acad. Sci. U.S.A. 93*, 8160−8166.
(42) Ito, Y., Yamasaki, K., Iwahara, J., Terada, T., Kamiya, A., Shirouzu, M., Muto, Y., Kawai, G., Yokoyama, S., Laue, E. D., Walchli, M., Shibata, T., Nishimura, S., and Miyazawa, T. (1997) Regional polysterism in the GTP-bound form of the human c-Ha-Ras protein. *Biochemistry 36*, 9109−9119.
(43) Stafford, A. J., Walker, D. M., and Webb, L. J. (2012) Electrostatic Effects of Mutation of Ras Glutamine 61 Measured using Vibrational Spectroscopy of a Thiocyanate Probe. *Biochemistry 51*, 2757−2767.
(44) Adams, P. D., Grosse-Kunstleve, R. W., Hung, L. W., Ioerger, T. R., McCoy, A. J., Moriarty, N. W., Read, R. J., Sacchettini, J. C., Sauter, N. K., and Terwilliger, T. C. (2002) PHENIX: Building new software for automated crystallographic structure determination. *Acta Crystallogr. D58*, 1948−1954.
(45) Emsley, P., and Cowtan, K. (2004) Coot: Model-building tools for molecular graphics. *Acta Crystallogr. D60*, 2126−2132.
(46) Shutes, A., and Der, C. J. (2005) Real-time in vitro measurement of GTP hydrolysis. *Methods 37*, 183−189.
(47) Monod, J., Changeux, J. P., and Jacob, F. (1963) Allosteric proteins and cellular control systems. *J. Mol. Biol. 6*, 306−329.
(48) Gunasekaran, K., Ma, B., and Nussinov, R. (2004) Is allostery an intrinsic property of all dynamic proteins? *Proteins 57*, 433−443.
(49) Kuriyan, J., and Eisenberg, D. (2007) The origin of protein interactions and allostery in colocalization. *Nature 450*, 983−990.
(50) Grant, B. J., McCammon, J. A., and Gorfe, A. A. (2010) Conformational selection in G-proteins: Lessons from ras and rho. *Biophys. J. 99*, L87−L89.
(51) O'Connor, C., and Kovrigin, E. L. (2008) Global conformational dynamics in ras. *Biochemistry 47*, 10244−10246.
(52) Spoerner, M., Herrmann, C., Vetter, I. R., Kalbitzer, H. R., and Wittinghofer, A. (2001) Dynamic properties of the Ras switch I region and its importance for binding to effectors. *Proc. Natl. Acad. Sci. U.S.A. 98*, 4944−4949.
(53) Spoerner, M., Wittinghofer, A., and Kalbitzer, H. R. (2004) Perturbation of the conformational equilibria in Ras by selective mutations as studied by ^{31}P NMR spectroscopy. *FEBS Lett. 578*, 305−310.
(54) McGuffee, S. R., and Elcock, A. H. (2010) Diffusion, crowding & protein stability in a dynamic molecular model of the bacterial cytoplasm. *PLoS Comput. Biol. 6*, e1000694.
(55) Vetter, I. R., Arndt, A., Kutay, U., Gorlich, D., and Wittinghofer, A. (1999) Structural view of the Ran-Importin β interaction at 2.3 Å resolution. *Cell 97*, 635−646.
(56) Oh, H. J., Lee, K. K., Song, S. J., Jin, M. S., Song, M. S., Lee, J. H., Im, C. R., Lee, J. O., Yonehara, S., and Lim, D. S. (2006) Role of the tumor suppressor RASSF1A in Mst1-mediated apoptosis. *Cancer Res. 66*, 2562−2569.
(57) Scheel, H., and Hofmann, K. (2003) A novel interaction motif, SARAH, connects three classes of tumor suppressor. *Curr. Biol. 13*, R899−R900.
(58) Liu, L., Tommasi, S., Lee, D. H., Dammann, R., and Pfeifer, G. P. (2003) Control of microtubule stability by the RASSF1A tumor suppressor. *Oncogene 22*, 8125−8136.
(59) Liu, L., Vo, A., and McKeehan, W. L. (2005) Specificity of the methylation-suppressed A isoform of candidate tumor suppressor RASSF1 for microtubule hyperstabilization is determined by cell death inducer C19ORF5. *Cancer Res. 65*, 1830−1838.
(60) Moshnikova, A., Frye, J., Shay, J. W., Minna, J. D., and Khokhlatchev, A. V. (2006) The growth and tumor suppressor NORE1A is a cytoskeletal protein that suppresses growth by inhibition of the ERK pathway. *J. Biol. Chem. 281*, 8143−8152.